IET Electrical Systems in Transportation

Research Article

IET Journals
The Institution of Engineering and Technology

State-of-charge and state-of-health estimation with state constraints and current sensor bias correction for electrified powertrain vehicle batteries

ISSN 2042-9738
Received on 9th June 2015
Revised on 14th November 2015
Accepted on 18th December 2015
doi: 10.1049/iet-est.2015.0030
www.ietdl.org

Pawel Malysz[1,2] ✉, Ran Gu[2], Jin Ye[3], Hong Yang[1,2], Ali Emadi[2]

[1]*Fiat Chrysler Automobiles, Electrified Propulsion Systems, Auburn Hills, MI, USA*
[2]*Department of Electrical and Computer Engineering, McMaster University, Hamilton, Canada*
[3]*Electrical Engineering, San Francisco State University, CA, USA*
✉ *E-mail: malyszp@mcmaster.ca*

Abstract: Pragmatic approaches are proposed to enhance battery state estimation using Kalman filter (KF) and extended KF. Notable novelties introduced include: the use of state/parameter constraints, asymmetric equivalent circuit model behaviour, inclusion of nominal models, and current sensor measurement bias estimation and compensation. The so-called delta parameters are estimated to handle cell variations, aging, and online deviation of parameters. Strategic simplifications that enable the use of traditional KF algorithm are described. Unique filter structures are presented for state-of-charge and state-of-health estimation, the latter focuses on capacity and impedance estimation. The performance of the proposed approaches is demonstrated on experimental drive-cycle data designed for electric vehicle (EV) and hybrid EV applications.

1 Introduction

Batteries are a fundamental component to enable clean, sustainable, and electrified transportation [1, 2]. A battery management system (BMS) manages the electric energy storage system in an electric vehicle (EV), hybrid EV (HEV), and plugin HEV (PHEV) [3]. The BMS monitors battery conditions and ensures healthy and safe operation of the battery. State estimation also plays a crucial role in the BMS. Three important states that need to be estimated are state-of-charge (SOC), state-of-health (SOH), and state-of-power (SOP). The SOC is analogous to the fuel gauge of conventional vehicles since it roughly indicates the percentage of remaining energy. SOH monitors phenomena such as cell impedance growth and capacity fade, both of which effect battery performance. The SOP is typically a measure of the maximum power output capabilities of the battery at any given point in time.

Online battery state estimation approaches using equivalent circuit modelling with algorithms based on least squares and derivatives of Kalman filter (KF) are popular. Recursive least squares (RLS) has been used by a number of researchers [4, 5]; these approaches rely on a linear-in-parameter model reformulation for use with the standard RLS algorithm. An advantage of this approach is only a single forgetting factor, that diminishes the influence of old data, needs to be tuned; a disadvantage is the need for nonlinear transformations to obtain the parameter of interest; these transformations can pose problematic numerical issues. Verbrugge and Koch [4] employed voltage-based RLS estimation of SOC as part of an approach that is weighted with current-based SOC estimation. Xiong *et al.* [5] have used RLS for both SOC and SOP estimation. To improve capacity estimation and its robustness, Plett [6] has proposed a modified RLS method referred to as a total least squares method; it considers input and output noises, such as accumulated ampere-hours and SOC. An SOC estimation approach based on using the open-circuit voltage (OCV) at various temperatures has been proposed by Xing *et al.* [7].

Many approaches based on extended KF (EKF) have been employed [8–13]. The non-linear relationship between the OCV and SOC forces the use of the EKF. The ability to embed the equivalent circuit model into the filter and inherent filter optimality associated with KF related approaches are two highlights of using EKF. A well-known disadvantage is non-trivial tuning of both process and measurement noise matrices. The seminal work by Plett [8] explored the use of EKF to estimate both SOC and model parameters. Both joint and dual EKF approaches were explored, the latter sacrifices some cross-correlation information in order to gain computational efficiency improvements. Methods to make the EKF more robust for SOC estimation have been proposed by He *et al.* [9]. Xiong *et al.* have recently proposed adaptive EKF approaches that automatically tune the filter online [10]. A similar adaptive EKF approach has been applied by Chen *et al.* [13]. Multi-scale dual EKF approaches have been recently proposed for the purpose of simultaneous SOC and capacity estimation [11, 12]. A fast timescale is used for SOC estimation and a slow timescale is used to estimate capacity.

Alternative filtering approaches have also been explored for battery state estimation. For example, a sigma-point KF (SPKF) was used by Plett [14] to simultaneously estimate SOC and model parameters. The SPKF mitigates some of the estimation bias that non-linearities introduce when using EKF. Gholizade-Narm and Charkhgard [15] employed a square-root unscented KF to improve numerical robustness of SOC estimation. To robustify SOC estimation Alfi *et al.* [16] employed and H-infinity filter with radial basis function-based neural networks. Zhang *et al.* [17] also employed an H-infinity filter to estimate SOC for HEV applications. Neural networks and unscented KF have been employed for SOC estimation by He *et al.* [18]. An extensive review of battery state estimation has been reported by Waag *et al.* [19].

In this paper, the contributions are as follows, pragmatic approaches are explored to improve battery state estimation using KF and EKF with the use of current sensor bias correction and parameter state constraints. A priori knowledge of state/parameter values can typically come in the form of inequality constraints, the inclusion of these is presented in this paper. The usage of constraints can bound estimated values to known ranges, e.g. non-negative resistances/capacities and known bounds for equivalent circuit models. This leads to more robust estimation. Modelling and calibration testing of fresh battery cells are routinely done during the design and production phase of electrified vehicles, therefore methods to incorporate nominal models into the estimation are also presented. The estimation of

deviations from this model called delta parameters are proposed, they can compensate for cell-to-cell variations and aging effects that cause time-varying parameters. An asymmetric equivalent circuit-based model that considers asymmetry in all resistances is introduced and is used for estimation. Rather than complicating the EKF, strategic simplifications are performed that allow the use of a linear model and the traditional KF. This is shown to be possible by using OCV as a state instead of SOC. Comparisons with KF and EKF are performed for both SOC and capacity estimation using unique joint filter structures and with drive cycle experimental data. A novel current sensor bias estimation filter based on a new voltage-input/current-output (VICO) cell model is presented. Finally, a method to incorporate this in a current bias compensation strategy for SOC and SOH estimation is also demonstrated.

The rest of the paper is organised as follows. Section 2 reviews algorithms for battery state estimation. Section 3 details the different models and filter structures. Section 4 presents the results of applying the proposed methods for SOC and SOH estimation on drive cycle data. Section 5 concludes the paper.

2 Estimation algorithms

2.1 Kalman filter

The KF embeds a model into the filter and uses it to predict an intermediate state estimate. A discrete-time state-space model of the following form is assumed

$$\boldsymbol{x}_k = \boldsymbol{A}_{k-1}\boldsymbol{x}_{k-1} + \boldsymbol{B}_{k-1}\boldsymbol{u}_{k-1} + \boldsymbol{w}_{k-1} \tag{1}$$

$$\boldsymbol{y}_k = \boldsymbol{C}_k\boldsymbol{x}_k + \boldsymbol{D}_k\boldsymbol{u}_k + \boldsymbol{v}_k \tag{2}$$

where $\boldsymbol{x}_k \in \Re^n$ is a to be estimated system state vector at time k and $\boldsymbol{u}_k \in \Re^p$ is a known input vector, $\boldsymbol{y}_k \in \Re^m$ a measurement vector, and $\boldsymbol{w}_k \in \Re^n$ and $\boldsymbol{v}_k \in \Re^m$ represent the process noise and measurement noise, respectively.

The KF is an optimal estimator [20] under the assumption of normally distributed, zero mean, and independent process and measurement noise, i.e. with probability distributions

$$P(\boldsymbol{w}) \sim \mathcal{N}(\boldsymbol{0}, \boldsymbol{Q}), \quad P(\boldsymbol{v}) \sim \mathcal{N}(\boldsymbol{0}, \boldsymbol{R}) \tag{3}$$

where $\boldsymbol{Q}$ is the process noise covariance and $\boldsymbol{R}$ is the measurement noise covariance. The mechanics of the KF are summarised in Table 1.

In the time update steps 1 and 2, a priori state and a priori covariance are predicted from time $k-1$ to time k. During the measurement update steps 3–5, the Kalman gain matrix $\boldsymbol{K}_k$ is used to obtain a posteriori covariance matrix and state estimate.

2.2 Extended KF

Consider a non-linear system of the form

$$\boldsymbol{x}_k = f(\boldsymbol{x}_{k-1}, \boldsymbol{u}_{k-1}) + \boldsymbol{w}_{k-1} \tag{4}$$

$$\boldsymbol{y}_k = g(\boldsymbol{x}_k, \boldsymbol{u}_k) + \boldsymbol{v}_k \tag{5}$$

Table 1 KF algorithm

Step	Equation
1. A priori covariance update	$\boldsymbol{P}_{k\|k-1} = \boldsymbol{A}_{k-1}\boldsymbol{P}_{k-1\|k-1}\boldsymbol{A}_{k-1}^{\mathrm{T}} + \boldsymbol{Q}_{k-1}$
2. A priori estimate prediction	$\hat{\boldsymbol{x}}_{k\|k-1} = \boldsymbol{A}_{k-1}\hat{\boldsymbol{x}}_{k-1\|k-1} + \boldsymbol{B}_{k-1}\boldsymbol{u}_{k-1}$
3. Kalman gain matrix calculation	$\boldsymbol{K}_k = \boldsymbol{P}_{k\|k-1}\boldsymbol{C}_k{}^{\mathrm{T}}(\boldsymbol{C}_k\boldsymbol{P}_{k\|k-1}\boldsymbol{C}_k^{\mathrm{T}} + \boldsymbol{R}_k)^{-1}$
4. A posteriori covariance update	$\boldsymbol{P}_{k\|k} = (\boldsymbol{I} - \boldsymbol{K}_k\boldsymbol{C}_k)\boldsymbol{P}_{k\|k-1}$
5. A posteriori estimate correction	$\hat{\boldsymbol{x}}_{k\|k} = \hat{\boldsymbol{x}}_{k\|k-1} + \boldsymbol{K}_k(\boldsymbol{y}_k - \boldsymbol{C}_k\hat{\boldsymbol{x}}_{k\|k-1} - \boldsymbol{D}_k\boldsymbol{u}_k)$

where $f()$ and $g()$ are non-linear functions, and $\boldsymbol{w}_k$ and $\boldsymbol{v}_k$ are process and measurement noise vectors, respectively. For such non-linear systems, a modified KF that linearises around the state estimates can be used. It is referred to as the EKF [20] and for non-linear systems it becomes a sub-optimal filter.

For EKF the non-linear functions of $f()$ and $g()$ are used for prediction, however covariance matrix updates and Kalman gain calculation employ linearised Jacobian matrices of $f()$ and $g()$ as follows

$$\boldsymbol{A}_k = \left.\frac{\partial f(\boldsymbol{x}, \boldsymbol{u}_k)}{\partial \boldsymbol{x}}\right|_{\boldsymbol{x}=\hat{\boldsymbol{x}}_{k|k}}, \quad \boldsymbol{C}_k = \left.\frac{\partial g(\boldsymbol{x}, \boldsymbol{u}_k)}{\partial \boldsymbol{x}}\right|_{\boldsymbol{x}=\hat{\boldsymbol{x}}_{k|k-1}} \tag{6}$$

The mechanics of the EKF are summarised in Table 2.

2.3 KF/EKF estimate projection with state constraints

When the state vector $\boldsymbol{x}_k$ is subject to linear time-varying equality constraints, $\boldsymbol{H}_k\boldsymbol{x}_k = \boldsymbol{h}_k$, the in-the-loop projection method proposed by Teixeira *et al.* [21] can be employed. It is assumed that $\boldsymbol{H}_k$ is a short full rank matrix. A weighted pseudoinverse denoted by $\boldsymbol{H}_k^+$ is obtained and used to project the state estimate vector and covariance matrix update. The mechanics of this approach are summarised in Table 3, Fig. 1 illustrates how this projection method can be integrated with the KF/EKF.

The projection method can also cover cases of inequality constraints $\boldsymbol{H}_k^{\mathrm{in}}\boldsymbol{x}_k \le \boldsymbol{h}_k^{\mathrm{in}}$ when an active set approach is employed [22]. An active set method uses the fact that it is only those constraints that are active at the solution of the problem that are significant. The active constraints can be represented by the equality constraint $\boldsymbol{H}_k\boldsymbol{x}_k = \boldsymbol{h}_k$, where the rows of $\boldsymbol{H}_k$ and $\boldsymbol{h}_k$ are the active subset of the rows of $\boldsymbol{H}_k^{\mathrm{in}}$ and $\boldsymbol{h}_k^{\mathrm{in}}$. Therefore, the linear inequality constraint problem becomes equivalent to the equality

Table 2 EKF algorithm

Step	Equation
1. A priori linearisation	$\boldsymbol{A}_{k-1} = \frac{\partial f(\boldsymbol{x}, \boldsymbol{u}_{k-1})}{\partial \boldsymbol{x}}\|_{\boldsymbol{x}=\hat{\boldsymbol{x}}_{k-1\|k-1}}$
2. A priori covariance update	$\boldsymbol{P}_{k\|k-1} = \boldsymbol{A}_{k-1}\boldsymbol{P}_{k-1\|k-1}\boldsymbol{A}_{k-1}^{\mathrm{T}} + \boldsymbol{Q}_{k-1}$
3. A priori estimate prediction	$\hat{\boldsymbol{x}}_{k\|k-1} = f(\hat{\boldsymbol{x}}_{k-1\|k-1}, \boldsymbol{u}_{k-1})$
4. A posteriori linearisation	$\boldsymbol{C}_k = \frac{\partial g(\boldsymbol{x}, \boldsymbol{u}_k)}{\partial \boldsymbol{x}}\|_{\boldsymbol{x}=\hat{\boldsymbol{x}}_{k\|k-1}}$
5. Kalman gain matrix calculation	$\boldsymbol{K}_k = \boldsymbol{P}_{k\|k-1}\boldsymbol{C}_k^{\mathrm{T}}(\boldsymbol{C}_k\boldsymbol{P}_{k\|k-1}\boldsymbol{C}_k^{\mathrm{T}} + \boldsymbol{R}_k)^{-1}$
6. A posteriori covariance update	$\boldsymbol{P}_{k\|k} = (\boldsymbol{I} - \boldsymbol{K}_k\boldsymbol{C}_k)\boldsymbol{P}_{k\|k-1}$
7. A posteriori estimate correction	$\hat{\boldsymbol{x}}_{k\|k} = \hat{\boldsymbol{x}}_{k\|k-1} + \boldsymbol{K}_k(\boldsymbol{y}_k - g(\hat{\boldsymbol{x}}_{k\|k-1}, \boldsymbol{u}_k))$

Table 3 Estimate projection algorithm

Step	Equation
1. Active linear constraints	$\boldsymbol{H}_k\boldsymbol{x}_k = \boldsymbol{h}_k$
2. Pseudoinverse calculation	$\boldsymbol{H}_k^+ = \boldsymbol{P}_{k\|k}\boldsymbol{H}_k^{\mathrm{T}}(\boldsymbol{H}_k\boldsymbol{P}_{k\|k}\boldsymbol{H}_k^{\mathrm{T}})^{-1}$
3. Covariance projection	$\boldsymbol{P}_{k\|k}^p = \boldsymbol{P}_{k\|k} - \boldsymbol{H}_k^+\boldsymbol{H}_k\boldsymbol{P}_{k\|k}\boldsymbol{H}_k^{\mathrm{T}}\boldsymbol{H}_k^{+^{\mathrm{T}}}$
4. Estimate projection	$\boldsymbol{x}_{k\|k}^p = \boldsymbol{x}_{k\|k} - \boldsymbol{H}_k^+(\boldsymbol{h}_k - \boldsymbol{H}_k\boldsymbol{x}_{k\|k})$

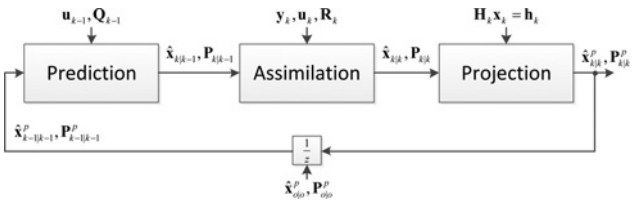

Fig. 1 *Algorithm with state estimate projection*

constraint problem when the active set is known a priori. It is noted numerical issues can arise since a rank deficient covariance matrix results, in [21] an *ad-hoc* solution is to add a small diagonal matrix to the covariance matrix after projection. Another *ad hoc* alternative is to ignore the covariance projection step altogether.

3 Battery state and parameter estimation

In this section, different battery state and parameter estimation methods and models are presented that employ the algorithms in Section 2. The different models are derived from a basic equivalent circuit model (ECM) that includes: an OCV that is a function of SOC [23], an ohmic resistance and RC elements that reflect the dynamics of the batteries. In this section, a model employing one RC element, as depicted in Fig. 2, is used as an example. Generalisation to higher order ECMs is straightforward [24]. SOC in this paper is defined as a number between zero and one representing the fraction of available Coulomb-counting capacity of the battery. SOH metrics are typically based on full-charge capacity and resistance, in this paper SOH generally refers to either of these parameters; explicit definitions of SOH metrics can be found in [3].

In Fig. 2, V_{oc} is the OCV, R_o is the ohmic resistance. V and I are the terminal voltage and terminal current, respectively. Positive current indicates discharging. R_a and C_a are the resistance and capacitance, respectively. I_a and V_a are the current through C_a and its voltage, respectively. The continuous time dynamics are

$$\dot{V}_a = -\frac{V_a}{R_a C_a} + \frac{I}{C_a} \tag{7}$$

$$V = V_{oc} - V_a - IR_o \tag{8}$$

In the subsequent subsections, approaches are presented to estimate battery SOC, impedance, capacity, and current bias. Inclusion of nominal model parameters and estimation of the deviations of these parameters are introduced as ways to improve filter performance. Rather than estimate SOC directly, the OCV V_{oc} is first estimated and then passed through an OCV–SOC look-up table to obtain SOC. Compensation of current bias is another method introduced to improve estimation performance. The overall battery state and parameter estimation strategy are summarised in Fig. 3. The remainder of this section will present filters that can be used for each of the separate estimation blocks shown in Fig. 3. Although different blocks may estimate some of the same parameters, tuning of each block can be done to optimise estimation of the state(s)/parameter(s) of interest.

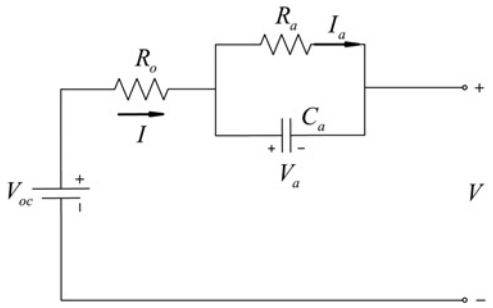

Fig. 2 *1RC equivalent circuit model*

3.1 Joint OCV and parameter estimation

3.1.1 EKF method – symmetric resistances: The vector to be estimated is $\boldsymbol{x} = [\theta, R_a, R_o, V_{oc}, V_a]^T$ where $\theta = e^{-(\Delta t/R_a C_a)}$. In this method, the state-space form is

$$\begin{bmatrix} \theta_k \\ R_{a,k} \\ R_{o,k} \\ V_{oc,k} \\ V_{a,k} \end{bmatrix} = \begin{bmatrix} \theta_{k-1} \\ R_{a,k-1} \\ R_{o,k-1} \\ V_{oc,k-1} \\ \theta_{k-1} V_{a,k-1} + R_{a,k-1}(1-\theta_{k-1}) I_{k-1} \end{bmatrix} + \boldsymbol{w}_{k-1} \tag{9}$$

$$V_k = V_{oc,k} - R_{o,k} I_k - V_{a,k} + v_k \tag{10}$$

The linearised Jacobian matrices of $f(\cdot)$ and $g(\cdot)$ to be used with

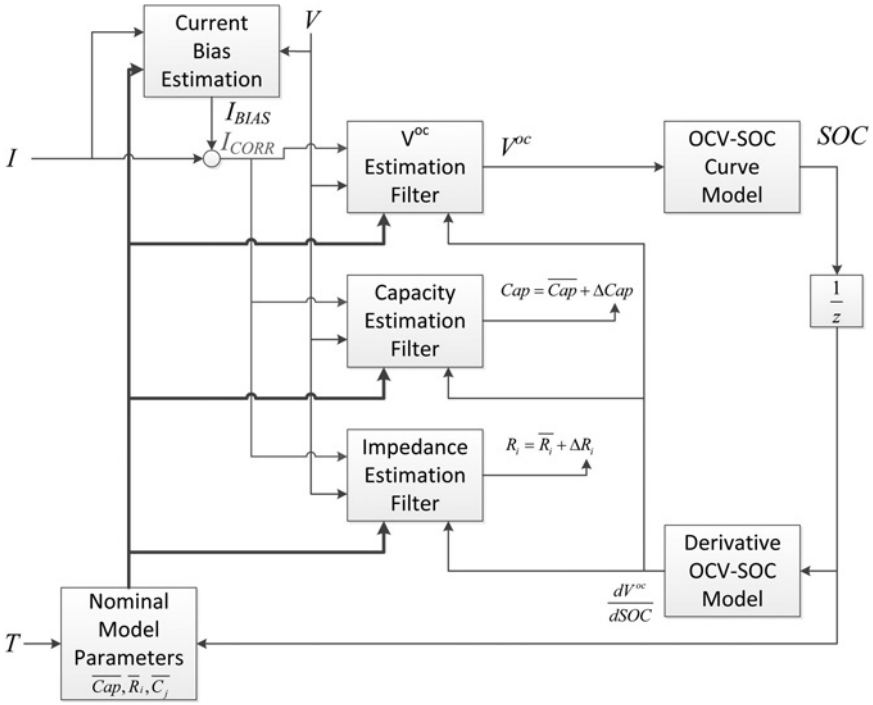

Fig. 3 *Battery SOC and SOH estimation strategy based on measurements of current (I), voltage (V), and temperature (T)*

IET Electr. Syst. Transp., 2016, Vol. 6, Iss. 2, pp. 136–144

EKF are

$$\boldsymbol{A}_k = \begin{bmatrix} 1 & 0 & 0 & 0 & 0 \\ 0 & 1 & 0 & 0 & 0 \\ 0 & 0 & 1 & 0 & 0 \\ 0 & 0 & 0 & 1 & 0 \\ V_{\mathrm{a},k} - R_{\mathrm{a},k} I_k & (1-\theta_k) I_k & 0 & 0 & \theta_{\mathrm{a},k} \end{bmatrix} \tag{11}$$

$$\boldsymbol{C}_k = \begin{bmatrix} -0 & 0 & -I_k & 1 & -1 \end{bmatrix}$$

3.1.2 EKF method – asymmetric resistances: In this approach, EKF is used to estimate the vector $\boldsymbol{x} = [\theta, R_{\mathrm{a}}^d, R_{\mathrm{a}}^c, R_{\mathrm{o}}^d, R_{\mathrm{a}}^c, V_{\mathrm{oc}}, V_{\mathrm{a}}]^{\mathrm{T}}$. The state-space form and Jacobian matrices are nearly identical to (9)–(11). The use of asymmetric resistance parameters and symmetric time-constants is motivated by analysis of high pulse power characterisation (HPPC) cell testing data. For some cells, it has been observed that the time constant parameter varies marginally between charge and discharge, moreover it has been observed this parameter also does not vary greatly over a wide SOC range. Resistances on the other hand have been observed to differ between charge and discharge current pulses. At low temperatures, cell resistance can also depend on the magnitude of the current.

3.2 Extensions to EKF/KF joint estimation

In this section, alternate filter models are presented intended to improve estimation performance. The first considers a model-based update in the OCV V_{oc} in a spirit analogous to current integration. This leads to the V_{oc} state to be modelled as

$$V_{\mathrm{oc},k} = V_{\mathrm{oc},k-1} - \frac{\mathrm{d}V_{\mathrm{oc},k-1}}{\mathrm{dSOC}_{k-1}} \cdot \frac{\Delta t}{\mathrm{CAP}} I_{k-1} \tag{12}$$

where CAP is the cell capacity; note the derivative of the OCV–SOC relationship is used here.

Another improvement is the inclusion of nominal model parameters and estimation of the deviation from these parameters. For example, each model parameter is divided into two parts: $R_{\mathrm{o}} = \bar{R}_{\mathrm{o}} + \widetilde{R}_{\mathrm{o}}$, $R_{\mathrm{a}} = \bar{R}_{\mathrm{a}} + \widetilde{R}_{\mathrm{a}}$, and $\theta = \bar{\theta} + \widetilde{\theta}$, where $\bar{R}_{\mathrm{o}}$, $\bar{R}_{\mathrm{a}}$, and $\bar{\theta}$ are nominal values that can be stored in look-up tables, and $\widetilde{R}_{\mathrm{o}}$, $\widetilde{R}_{\mathrm{a}}$, and $\widetilde{\theta}$ are denoted as delta parameters that are estimated on-line. Compared to the actual resistances themselves, the delta resistance parameters can be a more reliable estimate of impedance growth since their values should vary less due to their reduced dependence on operating conditions, e.g. SOC and temperature.

The third improvement is better described as a simplification to a time-varying KF. This is possible by eliminating the need to estimate θ and using a pre-described nominal value for it that can come from a look-up table. This approach lets the filter estimate the states and parameters of interest for SOC and SOH estimation, e.g. V_{oc} and delta resistances. This approach is motivated by the remarks in the previous section.

3.2.1 Delta EKF method – symmetric resistances: Using the aforementioned substitutions on model parameters the discrete-time model becomes

$$\begin{aligned} V_{\mathrm{a},k} &= (\bar{\theta} + \widetilde{\theta}) V_{\mathrm{a},k-1} + (\bar{R}_{\mathrm{a}} + \widetilde{R}_{\mathrm{a}})(1 - \bar{\theta} - \widetilde{\theta}) I_{k-1} \\ V_{\mathrm{oc},k} &= V_{\mathrm{oc},k-1} - \frac{\mathrm{d}V_{\mathrm{oc}}}{\mathrm{dSOC}} \cdot \frac{\Delta t}{\mathrm{CAP}} I_{k-1} \\ V_k &= V_{\mathrm{oc},k} - V_{\mathrm{a},k} - \bar{R}_{\mathrm{o}} I_k - \widetilde{R}_{\mathrm{o}} I_k \end{aligned} \tag{13}$$

The $V_{\mathrm{a},k}$ equation in (13) is a nonlinear function of estimation vector $\boldsymbol{x} = [\widetilde{\theta}, \widetilde{R}_{\mathrm{a}}, \widetilde{R}_{\mathrm{o}}, V_{\mathrm{oc}}, V_{\mathrm{a}}]^{\mathrm{T}}$ and terminal current I.

3.2.2 Delta EKF method – asymmetric resistances: Here asymmetric resistances are assumed and the following substitutions are made

$$R_{\mathrm{o}}^c = \bar{R}_{\mathrm{o}}^c + \widetilde{R}_{\mathrm{o}}^c, \quad R_{\mathrm{o}}^d = \bar{R}_{\mathrm{o}}^d + \widetilde{R}_{\mathrm{o}}^d \tag{14}$$

$$R_{\mathrm{a}}^c = \bar{R}_{\mathrm{a}}^c + \widetilde{R}_{\mathrm{a}}^c, \quad R_{\mathrm{a}}^d = \bar{R}_{\mathrm{a}}^d + \widetilde{R}_{\mathrm{a}}^d \tag{15}$$

where, $\bar{R}_{\mathrm{o}}^c$, $\bar{R}_{\mathrm{o}}^d$, $\bar{R}_{\mathrm{a}}^c$, and $\bar{R}_{\mathrm{a}}^d$ are the nominal values, and $\widetilde{R}_{\mathrm{o}}^c$, $\widetilde{R}_{\mathrm{o}}^d$, $\widetilde{R}_{\mathrm{a}}^c$, and $\widetilde{R}_{\mathrm{a}}^d$ are delta parameters to be estimated. The discrete-time model equations are

$$\begin{aligned} V_{\mathrm{a},k} &= (\bar{\theta} + \widetilde{\theta}) V_{\mathrm{a},k-1} + (\bar{R}_{\mathrm{a}}^d + \widetilde{R}_{\mathrm{a}}^d)(1 - \bar{\theta} - \widetilde{\theta}) I_{k-1}^+ \\ &\quad + (\bar{R}_{\mathrm{a}}^c + \widetilde{R}_{\mathrm{a}}^c)(1 - \bar{\theta} - \widetilde{\theta}) I_{k-1}^- \\ V_{\mathrm{oc},k} &= V_{\mathrm{oc},k-1} - \frac{\mathrm{d}V_{\mathrm{oc}}}{\mathrm{dSOC}} \cdot \frac{\Delta t}{\mathrm{CAP}} (I_{k-1}^+ + I_{k-1}^-) \\ V_k &= V_{\mathrm{oc},k} - V_{\mathrm{a},k} - \bar{R}_{\mathrm{o}}^d I_k^+ - \widetilde{R}_{\mathrm{o}}^d I_k^+ - \bar{R}_{\mathrm{o}}^c I_k^- - \widetilde{R}_{\mathrm{o}}^c I_k^- \end{aligned} \tag{16}$$

where $I_k^+ = \max(0, I_k)$ and $I_k^- = \min(0, I_k)$ are employed. The estimation vector is $\boldsymbol{x} = [\widetilde{\theta}, \widetilde{R}_{\mathrm{a}}^d, \widetilde{R}_{\mathrm{a}}^c, \widetilde{R}_{\mathrm{o}}^d, \widetilde{R}_{\mathrm{o}}^c, V_{\mathrm{oc}}, V_a]^{\mathrm{T}}$.

3.2.3 Delta KF methods: Non-linearity can be reduced in the filter by eliminating the estimation of the time-constant related parameter. A pre-described or nominal value can be used, i.e. $\theta = \bar{\theta}$. Two versions are considered. The first is the symmetric resistances model, the vector to be estimated is $\boldsymbol{x} = [\widetilde{R}_{\mathrm{a}}, \widetilde{R}_{\mathrm{o}}, V_{\mathrm{oc}}, V_a]^{\mathrm{T}}$. The discrete-time model simplifies to

$$\begin{aligned} V_{\mathrm{a},k} &= \theta V_{\mathrm{a},k-1} + \bar{R}_{\mathrm{a}}(1-\theta) I_{k-1} + \widetilde{R}_{\mathrm{a}}(1-\theta) I_{k-1} \\ V_{\mathrm{oc},k} &= V_{\mathrm{oc},k-1} - \frac{\mathrm{d}V_{\mathrm{oc}}}{\mathrm{dSOC}} \cdot \frac{\Delta t}{\mathrm{CAP}} I_{k-1} \\ V_k &= V_{\mathrm{oc},k} - V_{\mathrm{a},k} - \bar{R}_{\mathrm{o}} I_k - \widetilde{R}_{\mathrm{o}} I_k \end{aligned} \tag{17}$$

The result of eliminating θ from the state vector leads to the above equations to be linear time varying functions of estimation vector $\boldsymbol{x}_k$. It is straightforward to derive the matrices in (1) and (2) that are used by KF algorithm. Moreover, this improvement reduces the number of parameters to be estimated and concentrates the information the filter processes toward fewer estimated parameters.

A similar simplification can also be applied to the asymmetric resistances model. The vector to be estimated is $\boldsymbol{x} = [\tilde{R}_{\mathrm{a}}^d, \tilde{R}_{\mathrm{a}}^c, \tilde{R}_{\mathrm{o}}^d, \tilde{R}_{\mathrm{o}}^c, V_{\mathrm{oc}}, V_{\mathrm{a}}]^{\mathrm{T}}$. The discrete model equations used are

$$\begin{aligned} V_{\mathrm{a},k} &= \theta V_{\mathrm{a},k-1} + (\bar{R}_{\mathrm{a}}^d + \widetilde{R}_{\mathrm{a}}^d)(1-\theta) I_{k-1}^+ \\ &\quad + (\bar{R}_{\mathrm{a}}^c + \widetilde{R}_{\mathrm{a}}^c)(1-\theta) I_{k-1}^- \\ V_{\mathrm{oc},k} &= V_{\mathrm{oc},k-1} - \frac{\mathrm{d}V_{\mathrm{oc}}}{\mathrm{dSOC}} \cdot \frac{\Delta t}{\mathrm{CAP}} (I_{k-1}^+ + I_{k-1}^-) \\ V_k &= V_{\mathrm{oc},k} - V_{\mathrm{a},k} - \bar{R}_{\mathrm{o}}^d I_k^+ - \widetilde{R}_{\mathrm{o}}^d I_k^+ - \bar{R}_{\mathrm{o}}^c I_k^- - \widetilde{R}_{\mathrm{o}}^c I_k^- \end{aligned} \tag{18}$$

3.3 Joint capacity estimation

Another function of a BMS is to report the remaining useful energy in the battery, to accurately do this the full battery capacity, e.g. ampere-hour (Ah), has to be accurately known or estimated. Moreover, tracking capacity degradation is another metric for SOH estimation. Therefore KF and EKF approaches are derived to jointly estimate full battery capacity. Three different approaches are described in this subsection; they are essentially extensions of the approaches described in the previous subsections.

3.3.1 Delta EKF methods: Similar to the substitution of delta parameters in the previous section, capacity is divided into nominal parameter and delta parameter: $\mathrm{CAP} = \overline{\mathrm{CAP}} + \widetilde{\mathrm{CAP}}$. A nominal capacity $\overline{\mathrm{CAP}}$ can be defined as the initial cell capacity when the cell is new. A delta capacity parameter $\widetilde{\mathrm{CAP}}$ is

additionally estimated online. Applying this substitution to the delta EKF models of the previous subsection the $V_{\mathrm{oc},k}$ discrete-time equation is rewritten as

$$V_{\mathrm{oc},k} = V_{\mathrm{oc},k-1} - \frac{\mathrm{d}V_{\mathrm{oc}}}{\mathrm{dSOC}} \cdot \frac{\Delta t}{\overline{\mathrm{CAP}} + \widetilde{\mathrm{CAP}}} I_{k-1} \tag{19}$$

The estimation vectors are augmented with the additional estimate of delta capacity $\widetilde{\mathrm{CAP}}$. The delta parameter symmetric resistances version uses estimation vector $\boldsymbol{x}_k = [\widetilde{\mathrm{CAP}}, \tilde{\theta}, \tilde{R}_{\mathrm{a}}, \tilde{R}_{\mathrm{o}}, V_{\mathrm{oc}}, V_{\mathrm{a}}]^{\mathrm{T}}$, while the asymmetric resistances version employs $\boldsymbol{x}_k = [\widetilde{\mathrm{CAP}}, \tilde{\theta}, \tilde{R}^d_{\mathrm{a}}, \tilde{R}^c_{\mathrm{a}}, \tilde{R}^d_{\mathrm{o}}, \tilde{R}^c_{\mathrm{o}}, V_{\mathrm{oc}}, V_{\mathrm{a}}]^{\mathrm{T}}$.

3.3.2 Delta KF methods: Simplification to a KF is possible by eliminating estimation of θ and using the substitution $1/\mathrm{CAP} = (1/\overline{\mathrm{CAP}}) + i\widetilde{\mathrm{CAP}}$. A delta inverse capacity parameter is estimated. As long as the nominal value is non-zero the normality of the noise statistics of the delta capacity parameter is not greatly affected. The symmetric resistances version uses estimation vector $\boldsymbol{x}_k = [i\widetilde{\mathrm{CAP}}, \tilde{R}_{\mathrm{a}}, \tilde{R}_{\mathrm{o}}, V_{\mathrm{oc}}, V_{\mathrm{a}}]^{\mathrm{T}}$. The discrete time V_{oc} update equation becomes

$$V_{\mathrm{oc},k} = V_{\mathrm{oc},k-1} - \frac{\mathrm{d}V_{\mathrm{oc}}}{\mathrm{dSOC}} \cdot \Delta t(\overline{\mathrm{CAP}}^{-1} + i\widetilde{\mathrm{CAP}}) I_{k-1} \tag{20}$$

note the above equation is linear with respect to the estimation vector. The asymmetric resistances model uses estimation vector $\boldsymbol{x}_k = [i\widetilde{\mathrm{CAP}}, \tilde{R}^d_{\mathrm{a}}, \tilde{R}^c_{\mathrm{a}}, \tilde{R}^d_{\mathrm{o}}, \tilde{R}^c_{\mathrm{o}}, V_{\mathrm{oc}}, V_{\mathrm{a}}]^{\mathrm{T}}$ and V_{oc} update model

$$V_{\mathrm{oc},k} = V_{\mathrm{oc},k-1} - \frac{\mathrm{d}V_{\mathrm{oc}}}{\mathrm{dSOC}} \cdot \Delta t(\overline{\mathrm{CAP}}^{-1} + i\widetilde{\mathrm{CAP}}) \cdot (I^+_{k-1} + I^-_{k-1}) \tag{21}$$

3.4 VICO model with current bias estimation

The models presented thus far have been based on a current-input/voltage-output approach. This subsection derives a VICO discrete-time model. The approaches in this subsection use nominal values for the ECM parameters, e.g. resistances, capacitance, and capacity. This model is convenient since it is straightforward to augment it to include current bias estimation; this is also shown in this subsection.

3.4.1 KF using VICO model: The continuous-time model of a 1RC ECM can be expressed in state-space form as

$$\dot{\boldsymbol{x}} = \boldsymbol{A}\boldsymbol{x} + \boldsymbol{B}\boldsymbol{u}$$
$$\boldsymbol{y} = \boldsymbol{C}\boldsymbol{x} + \boldsymbol{D}\boldsymbol{u}$$

where the input, output, and states are defined as

$$\boldsymbol{y} = I, \quad \boldsymbol{x} = \begin{bmatrix} V_{\mathrm{a}} \\ V_{\mathrm{oc}} \end{bmatrix}, \quad \boldsymbol{u} = V$$

and the state-space matrices are

$$\boldsymbol{A} = \begin{bmatrix} \dfrac{-1}{R_{\mathrm{o}}C_{\mathrm{a}}} & -\dfrac{1}{R_{\mathrm{a}}C_{\mathrm{a}}} \\ 0 & \dfrac{1}{R_{\mathrm{o}}C_{\mathrm{a}}} \\ 0 & 0 \end{bmatrix}, \quad \boldsymbol{B} = \begin{bmatrix} \dfrac{-1}{R_{\mathrm{o}}C_{\mathrm{a}}} \\ 0 \end{bmatrix}$$
$$\boldsymbol{C} = \begin{bmatrix} \dfrac{-1}{R_{\mathrm{o}}} & \dfrac{1}{R_{\mathrm{o}}} \end{bmatrix}, \quad \boldsymbol{D} = \begin{bmatrix} \dfrac{-1}{R_{\mathrm{o}}} \end{bmatrix} \tag{22}$$

It is noted here that, for now, V_{oc} is assumed to be constant. Moreover, the relevant time-constant for such a system is

$$\frac{1}{\tau_{\mathrm{a||o}}} = \frac{1}{R_{\mathrm{o}}C_{\mathrm{a}}} + \frac{1}{R_{\mathrm{a}}C_{\mathrm{a}}} = \frac{R_{\mathrm{a}} + R_{\mathrm{o}}}{R_{\mathrm{a}}R_{\mathrm{o}}} \cdot \frac{1}{C_{\mathrm{a}}} \tag{23}$$

where it is evident that the relevant resistance is R_{o} in parallel with R_{a}.

For the purpose of continuous to discrete conversion, the discrete-time input, output, and states are defined as

$$\boldsymbol{y_k} = I_k, \quad \boldsymbol{x_k} = \begin{bmatrix} V_{a,k} \\ V_{\mathrm{oc},k} \end{bmatrix}, \quad \boldsymbol{u_k} = V_k$$

The discrete-time state-space matrices can be derived via a transfer function and inverse Laplace transform method [25], the result of which gives

$$\boldsymbol{A_k} = \mathrm{e}^{\boldsymbol{A}\overbrace{(t_k - t_{k-1})}^{\Delta t}} = \begin{bmatrix} \alpha & \dfrac{R_{\mathrm{a}}}{R_{\mathrm{a}} + R_{\mathrm{o}}}(1-\alpha) \\ 0 & 1 \end{bmatrix} \tag{24}$$

$$\boldsymbol{B_k} = \int_{t_{k-1}}^{t_k} \mathrm{e}^{\boldsymbol{A}(t_k - \tau)} \boldsymbol{B}\, \mathrm{d}\tau = \begin{bmatrix} \dfrac{R_{\mathrm{a}}}{R_{\mathrm{a}} + R_{\mathrm{o}}}(\alpha - 1) \\ 0 \end{bmatrix} \tag{25}$$

$$\boldsymbol{C_k} = \boldsymbol{C} = \begin{bmatrix} \dfrac{-1}{R_{\mathrm{o}}} & \dfrac{1}{R_{\mathrm{o}}} \end{bmatrix} \tag{26}$$

$$\boldsymbol{D_k} = \boldsymbol{D} = \begin{bmatrix} \dfrac{-1}{R_{\mathrm{o}}} \end{bmatrix} \tag{27}$$

$$\alpha = \mathrm{e}^{-\frac{\Delta t}{\tau_{\mathrm{a||o}}}} = \mathrm{e}^{-\frac{\Delta t(R_{\mathrm{a}} + R_{\mathrm{o}})}{C_{\mathrm{a}}R_{\mathrm{a}}R_{\mathrm{o}}}} \tag{28}$$

An alternative model can be derived by defining the input, output, and estimation vector to be

$$\boldsymbol{y}_k = I_k, \quad \boldsymbol{x}_k = \begin{bmatrix} \nu_k \\ V_{\mathrm{oc},k} \end{bmatrix}, \quad \boldsymbol{u}_k = V_k$$

where

$$\nu_k = V_{\mathrm{a},k}\frac{R_{\mathrm{a}} + R_{\mathrm{o}}}{R_{\mathrm{a}}}$$

is an internal state to be estimated. With this redefined state the discrete-time model equations become

$$\nu_k = \alpha\nu_{k-1} + (1-\alpha)V_{\mathrm{oc},k-1} + (\alpha - 1)V_{k-1} \tag{29}$$

$$V_{\mathrm{oc},k} = V_{\mathrm{oc},k-1} - \zeta \cdot \left(V_{\mathrm{oc},k-1} - \frac{R_{\mathrm{a}}}{R_{\mathrm{a}} + R_{\mathrm{o}}}\nu_{k-1} - V_{k-1}\right) \tag{30}$$

$$I_k = \frac{1}{R_{\mathrm{o}}}\left(V_{\mathrm{oc},k} - \frac{R_{\mathrm{a}}}{R_{\mathrm{a}} + R_{\mathrm{o}}}\nu_k - V_k\right) \tag{31}$$

where

$$\zeta = \frac{\mathrm{d}V_{\mathrm{oc}}}{\mathrm{d\,SOC}}\frac{\Delta t}{\mathrm{CAP}} \cdot \frac{1}{R_{\mathrm{o}}} \tag{32}$$

3.4.2 Current bias KF: It is commonplace for current sensors to exhibit measurement bias/offset; this ultimately biases SOC estimation and is extremely detrimental to capacity estimation. To compensate for current bias it can be added as an extra parameter to be jointly estimated. The output discrete-time (31) is straightforwardly modified as

$$I_k = \frac{1}{R_{\mathrm{o}}}\left(V_{\mathrm{oc},k} - \frac{R_{\mathrm{a}}}{R_{\mathrm{a}} + R_{\mathrm{o}}}\nu_k - V_k\right) + I_{\mathrm{bias}} \tag{33}$$

IET Electr. Syst. Transp., 2016, Vol. 6, Iss. 2, pp. 136–144

The input, output, and states are defined as

$$\boldsymbol{y}_k = I_k, \quad \boldsymbol{x}_k = \begin{bmatrix} v_k \\ V_{\mathrm{oc},k} \\ I_{\mathrm{bias}} \end{bmatrix}, \quad \boldsymbol{u}_k = V_k$$

It is assumed current bias is constant, therefore the state-space matrices used for its estimation via the KF are

$$\boldsymbol{A}_k = \begin{bmatrix} \alpha & (1-\alpha) & 0 \\ \dfrac{R_\mathrm{a}}{R_\mathrm{a}+R_\mathrm{o}}\zeta & 1-\zeta & 0 \\ 0 & 0 & 1 \end{bmatrix}, \quad \boldsymbol{B}_k = \begin{bmatrix} (\alpha-1) \\ \zeta \\ 0 \end{bmatrix} \tag{34}$$

$$\boldsymbol{C}_k = \begin{bmatrix} \dfrac{-1}{R_\mathrm{o}} \cdot \dfrac{R_\mathrm{a}}{R_\mathrm{a}+R_\mathrm{o}} & \dfrac{1}{R_\mathrm{o}} & 1 \end{bmatrix}, \quad \boldsymbol{D}_k = \begin{bmatrix} \dfrac{-1}{R_\mathrm{o}} \end{bmatrix}$$

With the above definitions the observability matrix $[\boldsymbol{C}, \boldsymbol{CA}, \boldsymbol{CA}^2]^\mathrm{T}$ is typically full rank, resulting in the three states being observable. A notable exception, that is not expected to be encountered, is when ζ is zero. This KF can be used solely for the purpose of current bias estimation to correct and compensate current measurements used in other estimation algorithms.

4 Estimation results

This section presents results for SOC and SOH estimation using the methods described in Section 3 with experimental measurements on Nickel-Manganese-Cobalt (NMC)-based lithium ion cells with a nominal capacity of 5.2 Ah. For each test a single cell has been excited using drive cycle profiles suitable for electrified vehicles. The cell response data has been provided by a major automotive Original Equipment Manufacturer (OEM). The cells were tested using a Maccor cell cycler and a Thermotron thermal chamber.

4.1 SOC estimation

SOC estimation performance is evaluated on cell response data that is appropriate for an EV application. The full range of cell SOC is considered along with a recharging segment. The methods presented in Section 3.2 are evaluated. Parameter estimation constraints are employed using the method described in Section 2.3. The constraints used are as follows, non-negativity of resistances and bounding estimation of $\theta = \mathrm{e}^{-\Delta t/R_\mathrm{a}(C_\mathrm{a})}$ to be $0.9 \leq \theta \leq 1$. The cell capacity has been measured a priori and was inputted in the estimation filters. The current and voltage input profiles for this scenario are shown in Fig. 4.

True SOC has been calculated using integration of current, measured capacity, and a known starting SOC point (Fig. 5). For the purpose of estimation, the voltage and current profiles have been contaminated with Gaussian noise with variances of 100 mA^2 and 2 mV^2 for current and voltage measurements, respectively. A comparison between the different methods is given in Fig. 6 where the mean and the maximum absolute error are shown.

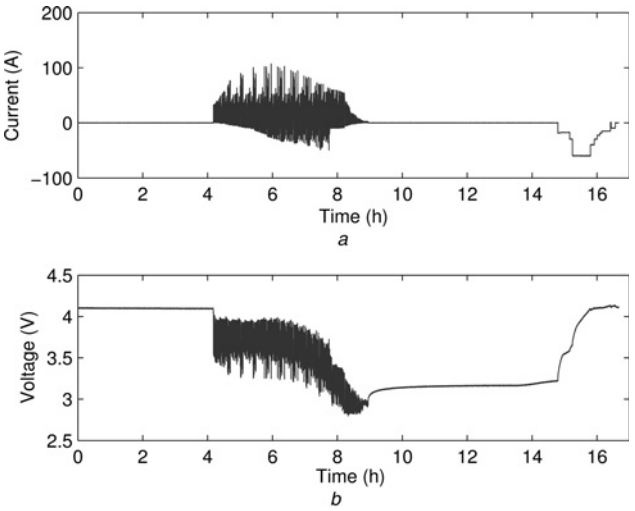

Fig. 4 *Full SOC range drive cycle and charging profiles*
a Current
b Voltage

From Fig. 6, it is seen that the use of an asymmetric resistance model outperforms a symmetric-based model for both KF and EKF. The use of constraints benefited the EKF approaches the most; EKF additionally estimated the time-constant related parameter θ. Nearly negligible marginal improvements for KF were observed using parameter constraints. The next scenario considers the effect of current measurement bias and the use of current bias estimation to compensate its effect. Current sensor bias of of 1 A was injected and was estimated using the filter in Section 3.4.2.

The output of the current bias KF performs best when current levels are low; this is expected since the sensitivity of current bias is greatest at low current levels. The output of the current bias KF was corrected to only except the KF estimation provided a sufficient low current time-period is satisfied, otherwise it would remember its old value. This approach proved to be effective. Fig. 7 shows the sensitivity of SOC to current measurement bias. Compared to Fig. 6 maximum errors nearly double for KF and approximately triple for EKF. The use of the proposed current bias compensation method greatly improves performance in all four cases.

4.2 SOH estimation

SOH estimation performance predominately in terms of capacity and some impedance estimation is described in this section. Three different Li-ion based cells have been cycled aged over a six month period using

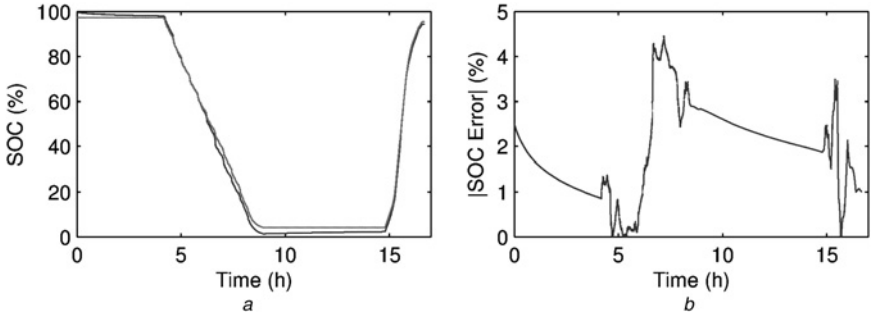

Fig. 5 *SOC and its estimation using KF with asymmetric resistances*
a SOC; true – grey line, estimate – black line
b Absolute value of SOC error

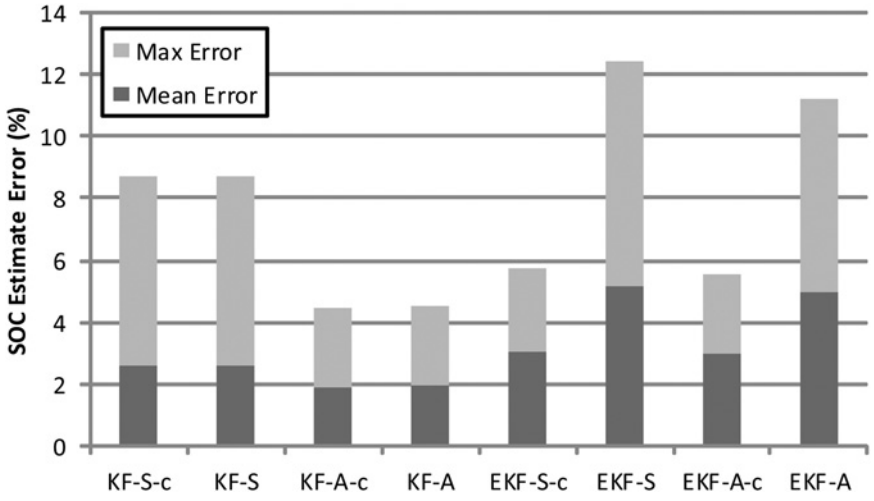

Fig. 6 *SOC estimation performance for an example full range SOC drive cycle. Note the '-c' indicates the usage of parameter constraints*

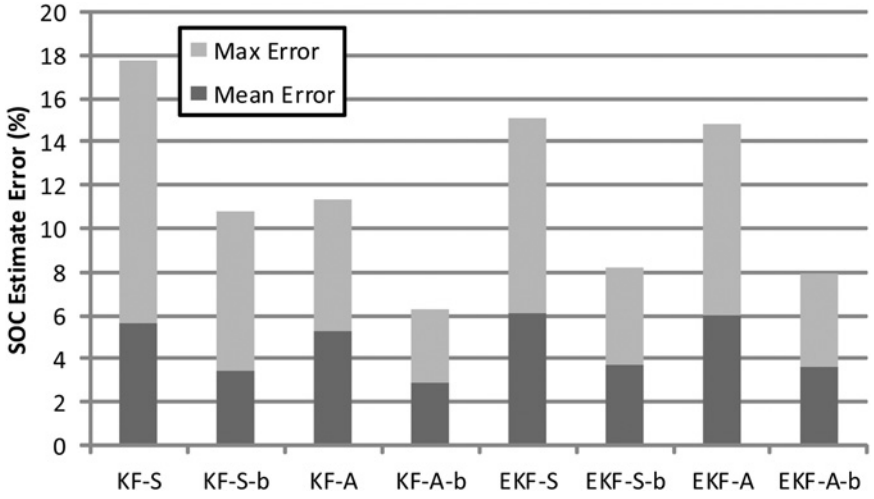

Fig. 7 *SOC estimation performance for an example full range SOC drive cycle with current measurement bias of 1 A. Note the '-b' indicates the usage of bias correction. All methods employ parameter constraints*

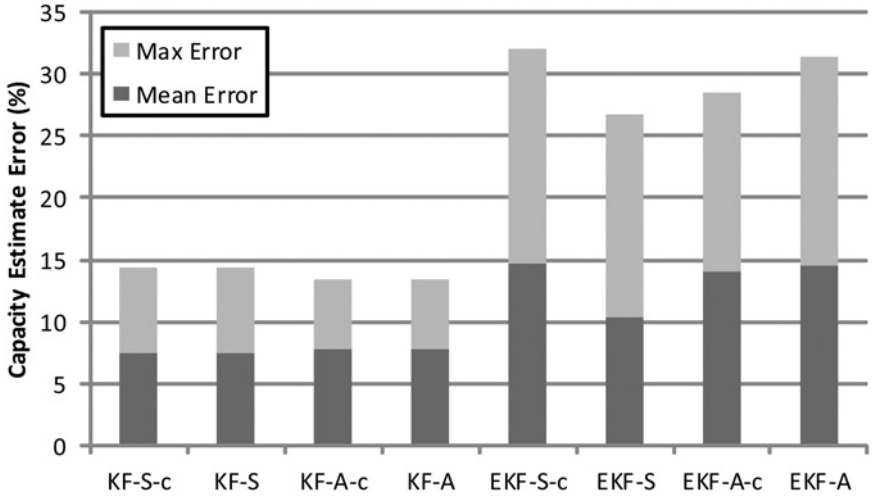

Fig. 8 *Capacity estimation performance for drive cycle aged cells. Note the '-c' indicates the usage of parameter constraints*

drive cycle profiles typical to an HEV application. Weekly data sets of cycled aged profiles were recorded. At three month intervals capacity measurements are performed, therefore nine different capacity measurements and weekly data sets were available; only the weekly profiles closest to the capacity measurement tests were used. The joint methods described in Section 3.3 were evaluated.

IET Electr. Syst. Transp., 2016, Vol. 6, Iss. 2, pp. 136–144

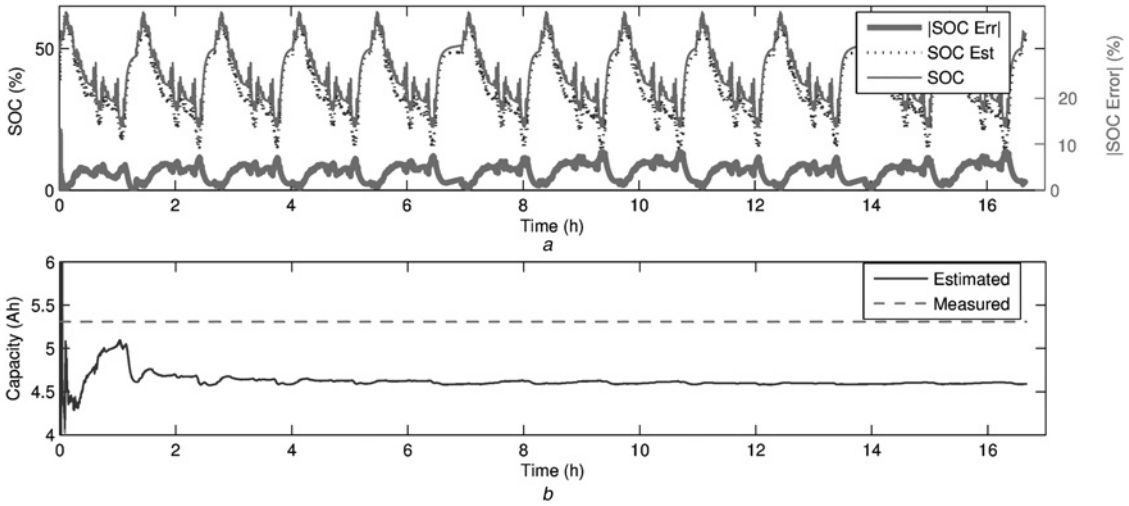

Fig. 9 *Sample results for joint SOC and capacity KF estimation using asymmetric resistances model*

a SOC (left *y*-axis) and absolute value of SOC error (right *y*-axis)
b Capacity

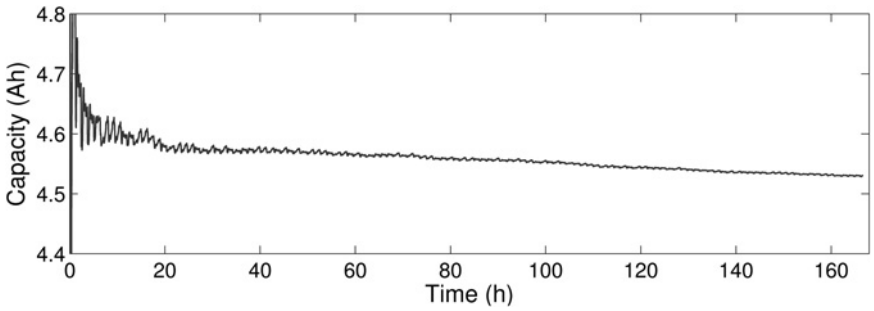

Fig. 10 *Capacity fade of drive-cycled aged sample cell over the course of one week*

The length of data used for each profile set was the first 60,000 s (16.66 h). The cycled aging repeats a combination of three commonly used automotive drive cycle profiles, between the repetitions a constant voltage charge to return the SOC to approximately 50% is performed. An HEV typical SOC operating range of approximately 30–70% was in effect. Since capacity degradation is typically a slow process, the last 5000 samples of capacity estimation were averaged and compared to the corresponding capacity measurement. The voltage/current measurements used by the KF/EKF were contaminated with the same noise as shown in Section 4.1; the same parameter constraints were also considered. Two estimation results were performed for each data set that used a nominal capacity value equal to the measured value ±10%. Therefore 18 capacity error measurements were available of which their mean and maximum absolute values are reported in Fig. 8.

The results depicted in Fig. 8 indicate the KF outperformed the EKF. The KF here had the advantage of estimating one less parameter compared to the EKF approaches. The capacity related filter structure for the EKF induced extra non-linearity that led to poorer global estimator performance of the EKF. There was no clear advantage of using an asymmetric resistance model and/or parameter constraints. A sample typical response for joint SOC and capacity estimation is illustrated in Fig. 9. The joint SOC–capacity estimation is used to estimate cell capacity fade without a full charge–discharge cycle, therefore is amenable to HEV, EV, and PHEV applications. Convergence of capacity estimation occurs within a few cycle repetitions, however in many cases an offset was observed that degraded the capacity estimation performance. Sources of this offset include an improperly calibrated and discretisation of the OCV–SOC curve [26]. Moreover, the OCV–SOC relation can slightly change as the battery ages inducing additional error in both SOC and capacity estimation.

Although the utility of absolute capacity estimation using joint KF/EKF has problems, their use for relative SOH metrics can be promising and can possibly be improved. Figs. 10 and 11 show sample results of capacity estimation and resistance estimation by extending the time range to a week to track capacity degradation. The asymmetric model KF was used. Minute capacity fade and resistance growth can be observed as the cell was cycle aged.

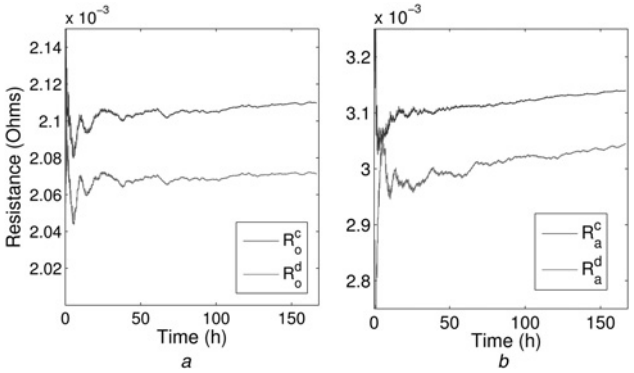

Fig. 11 *Resistance growth of drive-cycled aged sample cell over the course of one week*

a Ohmic resistance
b RC resistance

5 Concluding remarks

A multitude of practical improvements to battery state estimation using KF and EKF were presented and compared. These included: (i) in the loop state/parameter constraints, (ii) asymmetry in all resistances in the model, (iii) inclusion of nominal-parameter models, (iv) estimation of delta parameters, and (v) current sensor bias estimation and compensation. The above improvements were applied to filters designed to estimate SOC, and SOH metrics such as capacity and impedance. A joint estimation strategy was employed that used OCV as a system state rather than SOC. Useful simplifications were shown that enabled the use of the traditional KF algorithm.

Comparisons of the different filters and features were performed using experimental drive-cycle data. It was demonstrated that a KF using an asymmetric resistances model performed the best. State/parameter constraints were shown to improve SOC estimation, marginally for KF and significantly for EKF. However, significant improvements for capacity estimation using constraints were not observed. The detrimental effects of current sensor measurement bias on SOC estimation were shown, a method to substantially reduce this bias sensitivity was demonstrated via the use of a bias estimation filter. A new VICO model was employed for current bias estimation. For capacity estimation, KF-based methods were shown to be superior, the use of a symmetric resistances-based model showed similar performance to an asymmetric resistances-based model. The fundamental limitation of sensitivity to the derivative of the SOC–OCV curve on capacity estimation was shown to explain the typical estimation bias observed. The potential for relative SOH tracking was demonstrated by the ability to track small weekly changes in cell capacity and impedance. Future work will concentrate on multi-cell pack level estimation approaches and using improved models that handle resistance current magnitude dependency.

6 Acknowledgments

This research was undertaken thanks to funding and support from the Canada Excellence Research Chairs (CERC) Program, National Science and Engineering Research Council (NSERC) of Canada Automotive Partnership Canada (APC), and Fiat Chrysler Automobiles USA LLC and FCA Canada Inc.

7 References

1 Emadi, A.: 'Transportation 2.0', *IEEE Power Energy Mag.*., 2011, **9**, (4), pp. 18–29
2 Bilgin, B., Magne, P., Malysz, P., *et al.*: 'Making the case for electrified transportation', *IEEE Trans. Transp. Electrification*, 2015, **1**, pp. 4–17
3 Malysz, P.P., Gauchia, L., Yang, H.H.: 'Fundamentals of electric energy storage systems', *Adv. Electr. Drive Veh.*, 2014, pp. 237–282
4 Verbrugge, M., Koch, B.: 'Generalized recursive algorithm for adaptive multiparameter regression application to lead acid, nickel metal hydride, and lithium-ion batteries', *J. Electrochem. Soc.*, 2006, **153**, (1), pp. A187–A201
5 Xiong, R., He, H., Sun, F., *et al.*: 'Online estimation of peak power capability of li-ion batteries in electric vehicles by a hardware-in-loop approach', *Energies*, 2012, **5**, (5), pp. 1455–1469
6 Plett, G.L.: 'Recursive approximate weighted total least squares estimation of battery cell total capacity', *J. Power Sources*, 2011, **196**, (4), pp. 2319–2331
7 Xing, Y., He, W., Pecht, M., *et al.*: 'State of charge estimation of lithium-ion batteries using the open-circuit voltage at various ambient temperatures', *Appl. Energy*, 2014, **113**, pp. 106–115
8 Plett, G.L.: 'Extended Kalman filtering for battery management systems of lipb-based hev battery packs: Part 3 – state and parameter estimation', *J. Power Sources*, 2004, **134**, (2), pp. 277–292
9 He, H., Xiong, R., Fan, J.: 'Evaluation of lithium-ion battery equivalent circuit models for state of charge estimation by an experimental approach', *Energies*, 2011, **4**, (4), pp. 582–598
10 Xiong, R., Gong, X., Mi, C.C., *et al.*: 'A robust state-of-charge estimator for multiple types of lithium-ion batteries using adaptive extended Kalman filter', *J. Power Sources*, 2013, **243**, pp. 805–816
11 Xiong, R., Sun, F., Chen, Z., *et al.*: 'A data-driven multi-scale extended Kalman filtering based parameter and state estimation approach of lithium-ion polymer battery in electric vehicles', *Appl. Energy*, 2014, **113**, pp. 463–476
12 Hu, C., Youn, B.D., Chung, J.: 'A multiscale framework with extended Kalman filter for lithium-ion battery soc and capacity estimation', *Appl. Energy*, 2012, **92**, pp. 694–704
13 Chen, S., Gooi, H.B., Xia, N., *et al.*: 'Modelling of lithium-ion battery for online energy management systems', *IET Electr. Syst. Transp.*, 2012, **2**, (4), pp. 202–210
14 Plett, G.L.: 'Sigma-point Kalman filtering for battery management systems of lipb-based hev battery packs: part 2: simultaneous state and parameter estimation', *J. Power Sources*, 2006, **161**, (2), pp. 1369–1384
15 Gholizade-Narm, H., Charkhgard, M.: 'Lithium-ion battery state of charge estimation based on square-root unscented Kalman filter', *IET Power Electron.*, 2013, **6**, (9), pp. 1833–1841
16 Alfi, A., Charkhgard, M., Zarif, M.H.: 'Hybrid state of charge estimation for lithium-ion batteries: design and implementation', *IET Power Electron.*, 2014, **7**, (11), pp. 2758–2764
17 Zhang, Y., Zhang, C., Zhang, X.: 'State-of-charge estimation of the lithium-ion battery system with time-varying parameter for hybrid electric vehicles', *IET Control Theory Appl.*, 2013, **8**, (3), pp. 160–167
18 He, W., Williard, N., Chen, C., *et al.*: 'State of charge estimation of lithium-ion batteries using neural network modeling and unscented Kalman filter-based error cancellation', *Int. J. Electr. Power Energy Syst.*, 2014, **62**, pp. 783–791
19 Waag, W., Fleischer, C., Sauer, D.U.: 'Critical review of the methods for monitoring of lithium-ion batteries in electric and hybrid vehicles', *J. Power Sources*, 2014, **258**, pp. 321–339
20 Bishop, G., Welch, G.: 'An introduction to the Kalman filter', *Proc of SIGGRAPH, Course*, 2001, **8**, pp. 27599–3175
21 Teixeira, B.O., Chandrasekar, J., Tôrres, L.A., *et al.*: 'State estimation for linear and non-linear equality-constrained systems', *Int. J. Control*, 2009, **82**, (5), pp. 918–936
22 Simon, D.: 'Kalman filtering with state constraints: a survey of linear and nonlinear algorithms', *IET Control Theory Appl.*, 2010, **4**, (8), pp. 1303–1318
23 Pei, L., Lu, R., Zhu, C.: 'Relaxation model of the open-circuit voltage for state-of-charge estimation in lithium-ion batteries', *IET Electr. Syst. Transp.*, 2013, **3**, (4), pp. 112–117
24 Hsieh, Y.-C., Lin, T.-D., Chen, R.-J., *et al.*: 'Electric circuit modelling for lithium-ion batteries by intermittent discharging', *IET Power Electron.*, 2014, **7**, (10), pp. 2672–2677
25 Chen, C.-T.: 'Linear system theory and design' (Oxford University Press, Inc., 1998)
26 Wang, W., Ye, J., Malysz, P., *et al.*: 'Sensitivity analysis of Kalman filter based capacity estimation for electric vehicles'. IEEE Transportation Electrification Conf. and Expo (ITEC), 2015